Available online at www.sciencedirect.com
ScienceDirect
Surface Science 601 (2007) 5740–5743
SURFACE SCIENCE
www.elsevier.com/locate/susc

Characterisation of alkyl-functionalised Si(1 1 1) using reflectometry and AC impedance spectroscopy

Elicia L.S. Wong [a,b], Michael James [a,*], Terry C. Chilcott [b], Hans G.L. Coster [b]

[a] *Australian Nuclear Science and Technology Organisation, Lucas Heights Research Laboratory, Lucas Height, NSW 2234, Australia*
[b] *Biophysics and Bioengineering, School of Chemical and Biomolecular Engineering, University of Sydney, NSW 2008, Australia*

Available online 5 July 2007

Abstract

The past few years have seen a dramatic increase in the study of organic thin-film systems that are based on silicon–carbon covalent bonds for bio-passivation or bio-sensing applications. This approach to functionalizing Si wafers is in contrast to gold-thiol or siloxane chemistries and has been shown to lead to densely packed alkyl monolayers. In this study, a series of alkyl monolayers [$CH_3(CH_2)_nCH{=}CH_2$; $n = 7, 9, 11, 13, 15$] were directly covalent-linked to Si(1 1 1) wafers. The structures of these monolayers were studied using X-ray reflectometry (XRR) and AC impedance spectroscopy. Both techniques are sensitive to the variation in thickness with each addition of a CH_2 unit and thus provide a useful means for monitoring molecular-scale events. The combination of these techniques is able to probe not only the thickness, but also the interfacial roughness and capacitance of the layer at the immobilized surface with atomic resolution. Fundamental physical properties of these films such as chain canting angles were also determined.

Keywords: X-ray reflectometry; AC impedance spectroscopy; Self-assembled monolayer; Thin film

1. Introduction

Molecular self-assembly is a powerful approach for producing novel nanoscale architectures at the solid surfaces. To date self-assembled monolayers (SAMs) utilizing thiol-bonds to gold and organosilanes on silica surfaces have been used extensively for the controlled immobilisation of biomolecules. Regardless of the substrates and strategies being used to form SAMs a detailed understanding of the structure, molecular packing, and surface termination of these films is essential for understanding the relationships between microscopic structure and macroscopic chemical and physical properties. Different analytical techniques, including X-ray photoelectron spectroscopy (XPS) [1], ellipsometry [2], transmission electron microscopy (TEM) [3], atomic force microscopy (AFM) [4,5] and scanning tunneling microscopy (STM) [6,7] have been used and provide an excellent basis for the understanding of the structure, order and bonding of SAMs. Nevertheless, the ability to monitor the effect of changes in molecular structure at the SAMs upon biorecognition events is also vital to give an insight to the fundamental chemistries taking place at the interface.

In this study, we apply the scattering technique of X-ray reflectometry (XRR) and the electrochemical technique of AC impedance spectroscopy to investigate a series of alkyl monolayers [$CH_3(CH_2)_nCH{=}CH_2$; $n = 7, 9, 11, 13, 15$], which were covalently bonded to the surface of Si(1 1 1) wafers. Henceforth these will be referred to as C10, C12, C14, C16, and C18 organic monolayers. Both XRR and AC impedance techniques are non-destructive and non-contact techniques; however the XRR is performed in the air while the impedance measurements are performed in aqueous solution. Our objective is to take advantage of the high surface sensitivity of both techniques to show that complementary information, such as the thicknesses of these monolayers can be obtained with angstrom precision.

* Corresponding author. Tel.: +61 2 9717 9299; fax: +61 2 9717 3606.
E-mail address: mja@ansto.gov.au (M. James).

0039-6028/$ - see front matter © 2007 Elsevier B.V. All rights reserved.
doi:10.1016/j.susc.2007.06.067

2. Experimental procedure

2.1. Materials

Reagent grade 1-decene, 1-dodecene, 1-tetradecene, 1-hexadecene, 1-octadecene, potassium chloride, dichloromethane and methanol were purchased from Aldrich Chemicals (Sydney, NSW, Australia). Hydrogen peroxide, concentrated sulphuric acid and absolute ethanol were purchased from Ajax (Sydney, Australia). 40% ammonium fluoride was obtained from Kanto Kagaku Singapore Pty Ltd. (Singapore). All the chemicals were used as received without further purification. Milli-Q (18 MΩ cm) was used for the rinsing and preparation of solutions.

2.2. Preparation of Si–C linked monolayers

Highly doped Si(1 1 1) wafer pieces (n-type, 0.01–0.1 Ω cm) were cleaned using "Piranha" solution (concentrated H_2SO_4:30% H_2O_2, 3:1, v/v) at 90 °C for 30 min and rinsed thoroughly with Milli-Q water. Caution: piranha solution is highly oxidizing and should be used with extreme care. The process of surface functionalisation of Si wafers by *n*-alkenes follows the method by Sieval et al. [8] and is summarised in Scheme 1 and proceeds as follows. The hydrogen-terminated Si(1 1 1) surfaces were prepared by etching the cleaned Si(1 1 1) wafer in deoxygenated 40% ammonium fluoride solution for 20 min. The 40% ammonium fluoride solution was deoxygenated by bubbling with nitrogen for 30 min. The freshly etched Si(1 1 1) wafers were then functionalized by hydrosilylation *via* thermal activation in neat alkene solution. The neat *n*-alkene (liquid) was deoxygenated by bubbling with nitrogen for 30 min and was placed into a Schlenk flask. The freshly etched Si(1 1 1)-H wafer was then added and the flask heated in an oil bath for 3 h at 200 °C under vacuum (2 mbar). After the reaction the cooled flask was opened to the atmosphere and the functionalized silicon wafer was rinsed with hexane, dichloromethane, tetrahydrofuran and ethanol and dried thoroughly under a stream of nitrogen.

2.3. X-ray reflectometry

X-ray reflectivity curves were acquired using a Panalytical Ltd. X'Pert Pro diffractometer in reflectometer mode. Cu Kα ($\lambda = 1.5406$ Å) radiation produced from a (45 kV) tube source was focused with a Göbel mirror, collimated with pre-and post-sample slits, and detected using a NaI scintillator detector. Reflectivity data are presented as a function of momentum transfer $Q_z = 4\pi \sin\theta/\lambda$, where λ is the X-ray wavelength and θ the angle of incidence onto the sample. Data were collected over the range $0.03° \leqslant \theta \leqslant 5.00°$ in 0.01° steps with counting times of 20 s per step. The Parratt32 software [9] was used to fit model parameters to measured sets of X-ray reflectivity data with a constant background correction. Low frequency oscillations (Kiessig fringes) were observed as expected for a Si surface functionalized by an organic monolayer, which are normally observed for a surface modified with a thin film on a solid substrate.

2.4. AC impedance measurements

AC impedance measurements were performed using an INPHAZE Pty Ltd impedance spectrometer. The 3-terminal measurements were carried out using a 3-electrode system in 100 mM potassium chloride solution, with Ag|AgCl as the reference electrode, platinum as the counter electrode and functionalized Si(1 1 1) wafer as the working electrode. Gallium–indium eutectic was applied to form a rear ohmic contact to the silicon wafers. For the current experiments, the capacitances of the SAMs were measured at a frequency of 0.558 Hz. It has been established from previous studies [10–12] that at this frequency the measured capacitance reflects the capacitance of the layer with the lowest conductance; the strong dispersion in capacitance due to the electrolyte in series with the sample does not manifest for frequencies below ~1000 Hz. The low frequency capacitance is related to the thickness, *d*, of the layers by:

$$d = \frac{\varepsilon_l \varepsilon_o}{C},$$

where ε_l is the dielectric constant of the organic layer, ε_o is the permittivity of free space ($=8.85 \times 10^{-12}$), *C* is the capacitance per unit area.

3. Results and discussion

3.1. XRR measurements

Observed (crosses) and fitted (solid lines) XRR curves for a series of Si(1 1 1) surfaces functionalized with C10, C12, C14, C16, and C18 covalently-linked monolayers

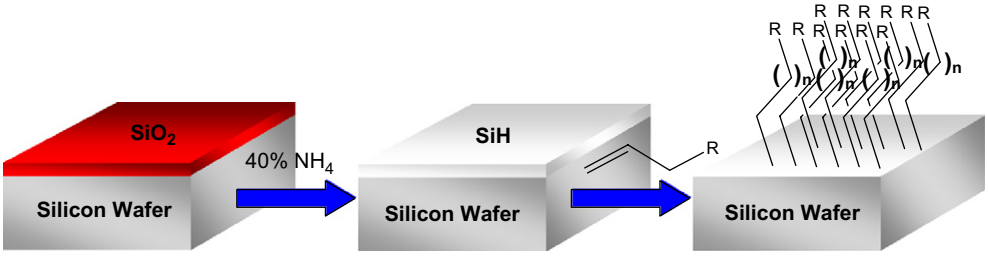

Scheme 1. Schematic representation of the reaction of 1-alkene with a hydrogen-terminated silicon surface.

are shown in Fig. 1. Unlike the smooth Fresnel decay of a bare Si(1 1 1)-H surface , the XRR curves for these monolayers show the minima of the first Kiessig fringes. Pomerantz et al. [13] and Linford et al. [14] have also observed a similar minima for octadecyltrichlorosilane monolayers on oxidized silicon [13] and an octadecyl monolayer on Si(1 1 1) [14]. The measured reflectivity for each of these monolayers varied over seven orders of magnitude before the background was reached. Even prior to modelling, the shift in position of the minima towards lower Q_z clearly demonstrates the increase in the thickness of these organic monolayers with increasing alkyl chain length (Fig. 1).

Reflectivity data for C10–C18 monolayers were fitted using a single layer model. The refined monolayer thickness and roughness of the monolayer/substrate and monolayer/air interfaces based on these fitted reflectivity data are given in Table 1. The thicknesses of the C10, C12, C14, C16, and C18 Si–C linked monolayers were found to be 10(1), 13(1), 16(1), 19(1) and 22(1) Å, respectively, where a clear linearity is observed as expected for this series of alkyl chains. Each methylene group adds approximately 1.5 Å to the monolayer thickness, which is in good agreements with the thicknesses of alkyl monolayers obtained on Si(1 0 0) and Si(1 1 1) using XRR. Sieval et al. [8] for example reported a thickness of 20 Å for a octadecyl monolayer on Si(1 1 1); while Rozlosnik et al. [15] have characterised a SAM of octadecyltrichlorosilane on Si(0 0 1) at 25 Å. These, along with our own results, appear to be typically 2–3 Å shorter than previously reported alkyl layers on gold substrates. Graupe et al. [16] reported a thickness of 19.5 Å for a hexadecyl monolayer on gold that was thermally evaporated onto Si(1 0 0) surface; while Linford and Chidsey [17] reported a 17 Å for a dodecyl monolayer on gold. Regardless the substrate used for SAMs formation, the thickness of these alkyl monolayers is shorter than the calculated length of fully stretched alkyl chain (aligned normal to the surface).

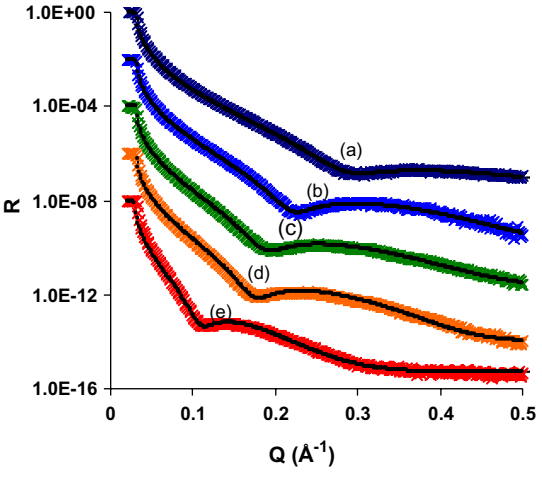

Fig. 1. XRR curves for Si–C linked monolayers of (a) C10, (b) C12, (c) C14, (d) C16, and (e) C18 alkyl chain lengths. Each curve is offset by 10^{-2} for clarity. The crosses represent the observed data while the solid lines represent model fits to these data.

The refined values for interfacial roughness (σ) of the Si/monolayer and monolayer/air interfaces are effectively constant within the estimated standard deviations across the series. There is some suggestion that the upper monolayer/air surface of the longer (C14–C18) alkyl chains are smoother than the 4 Å of the underlying Si substrates. This may be due to their ability pack in a more flexible manner.

Tilting of alkyl chains from surface normal has been previously well documented for these types of self-assembled systems [20,21], and was also observed for all of the samples measured in this study. The canting angles with respect to surface normal ranged between 37(2)° and 41(2)° for our alkyl monolayers on Si(1 1 1) (Table 1) and are in good agreement with other reported values for alkyl monolayers on Si(1 1 1) and Si(1 0 0) surfaces. Linford et al. [14] reported a cant angle of 36° for an octadecyl monolayers formed on Si(1 1 1) surface. This value is also similar to that of analogous chain length thiols on gold [18] and theoretical calculations also indicate that a ~30–38° canting angles on gold minimizes the energy for these surfaces [19].

3.2. AC impedance measurements

The AC impedance measurements for the Si–C linked monolayer were performed in 100 mM potassium chloride solution *via* 3-electrode measurement. Fig. 2 shows that the measured capacitance (□) decreases with increasing number of carbon atoms of the n-alkyl monolayer on the Si(1 1 1) surface. This trend is also consistent with Yu et al. [21], where a decrease in capacitance was observed for different chain lengths where $n = 2$, 6, 10 and 15 when in contact with 0.1 M H_2SO_4 + 2% HF. Fig. 2 also shows that the thickness (■) of these *n*-alkyl monolayers ($n = 10$, 12, 14, 16 and 18) increases linearly with n (1.26 Å/atom with correlation efficient of 0.9991) and are in excel-

Table 1
Refined thickness (d) and interfacial roughness parameters (σ) for Si(1 1 1) functionalised with monolayers of C10, C12, C14, C16, and C18 from X-ray reflectivity measurements

Monolayer	C10	C12	C14	C16	C18
d (Å)[a]	10(1) *11.8(2)*	13(1) *14.1(2)*	16(1) *16.6(2)*	19(1) *19.3(5)*	22(1) *22.4(8)*
σ (Å)-monolayer/air	4(1)	4(1)	3(1)	2(1)	2(1)
σ (Å)-Si/monolayer	4(1)	4(1)	4(1)	4(1)	4(1)
Canting angle to normal (°)[a]	41(3)	41(2)	39(2)	37(2)	38(2)

[a] Values in italics are those determined from AC impedance spectroscopy (Fig. 2).

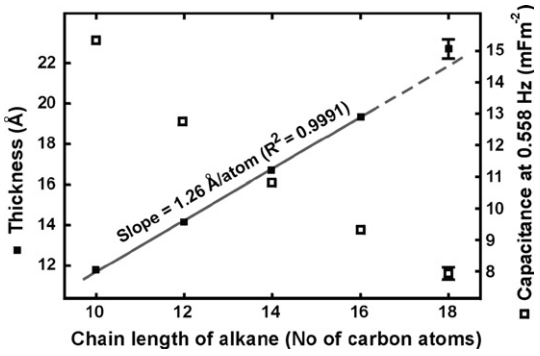

Fig. 2. Capacitance and thickness of at n-alkyl monolayers modified Si(1 1 1)/100 mM potassium chloride plots as a function of the number carbon atoms. The solid line is a least-squares fit to the experimental data.

lent agreement with the XRR results. These values were determined assuming a dielectric constant (ε) of 2.05, which is the accepted range for polyethylene [22]. Our results also verifies the correlation between the thickness and the capacitive properties of the *n*-alkyl monolayers and is consistent with the interfacial capacitive measurement obtained for alkanethiol monolayers on gold [18,23]. The correlation for *n*-alkyl monolayer on silicon (Fig. 2) is definitive for $n = 10$, 12, 14 and 16 but diverges slightly for larger n (i.e. $n = 18$), which is consistent with the orientation of the longer chain monolayer approaching closer to the surface normal [24].

3.3. Comparison between XRR and AC impedance

Examination of Table 1 as well as Figs. 1 and 2 reveals that both techniques give excellent discrimination in *n*-alkyl chain length measurement as a function of the number of carbon atoms. In absolute terms, the agreement between these two very different techniques becomes better with increasing chain length. This may in part be due to the relatively lower sensitivity of XRR for the shortest chain lengths. As the first minima in the XRR data moves to higher Q for thinner films, the ability to clearly distinguish it against the instrumental background becomes increasingly difficult. The XRR data for the 10 Å thick $C_{10}H_{21}$ chain does show a clear minima at $Q \sim 0.3$ Å^{-1}, although this is almost at the limit that can be detected using a laboratory-based instrument. The value of 11.8 Å determined by AC impedance is for example closer in value to the 11.5 Å determined by Cheng et al. [25].

4. Conclusion

Different *n*-alkyl monolayers ($n = 10$, 12, 14, 16 and 18) were functionalized on Si(1 1 1) surfaces through hydrosilylation *via* thermal activation under vacuum. These monolayers were characterized using both XRR and AC impedance measurements. Both the XRR and AC impedance spectroscopy demonstrated the ability to probe the structure of these functionalized monolayers with angstrom precision and the thickness values obtained from both techniques are in good agreement with one another. In addition to monolayer thickness, chain canting angle and interfacial roughness information such as film density and molecular footprint of these monolayers can also be acquired from these distinctive and yet complementary techniques. These latter parameters do however require a substantially more complex frequency dispersive measurement and analysis protocol; particularly in regards to the AC impedance spectroscopy. None-the-less, both techniques do provide an excellent means of monitoring molecular-scale events at solid and solid-solution interfaces.

Acknowledgement

We would like to thank Australian Research Council (ARC) for the funding of this research (Discovery Grant Number: DP0452447).

References

[1] D.A. Hutt, G.J. Leggett, Langmuir 13 (1997) 3055.
[2] A.N. Parikh, B. Liedberg, S.V. Atre, M. Ho, D.L. Allara, J. Phys. Chem. 99 (1995) 9996.
[3] L. Strong, G.M. Whitesides, Langmuir 4 (1988) 546.
[4] J. Pan, N. Tao, S.M. Lindsay, Langmuir 9 (1993) 1556.
[5] H.I. Kim, T. Koini, T.R. Lee, S.S. Perry, Langmuir 13 (1997) 7192.
[6] G.E. Poirier, Chem. Rev. 97 (1997) 1117.
[7] G.E. Poirier, M.J. Tarlov, Langmuir 10 (1994) 2853.
[8] A.B. Sieval, A.L. Demirel, J.W.M. Nissink, M.R. Linford, J.H. van der Mass, W.H. de Jeu, H. Zuilhof, E.J.R. Sudholter, Langmuir 14 (1998) 1759.
[9] C. Braun, Neutron Scattering Center, Hahn Meitner Institute, Berlin, 1999.
[10] T.C. Chilcott, M. Chan, L. Gaedt, T. Nantawisarakul, A.G. Fane, H.G.L. Coster, J. Membrane Sci. 195 (2002) 153.
[11] L. Gaedt, T.C. Chilcott, M. Chan, T. Nantawisarakul, A.G. Fane, H.G.L. Coster, J. Membrane Sci. 195 (2002) 169.
[12] H.G.L. Coster, T.C. Chilcott, A.C.F. Coster, Bioelectroch. Bioener. 40 (1996) 79.
[13] M. Pomerantz, A. Segmuller, L. Netzer, J. Sagiv, Thin Solid Films 132 (1985) 153.
[14] M.R. Linford, P. Fenter, P.M. Eisenberger, C.E.D. Chidsey, J. Am. Chem. Soc. 117 (1995) 3145.
[15] N. Rozlosnik, M.C. Gerstenberg, N.B. Larsen, Langmuir 19 (2003) 1182.
[16] M. Graupe, T. Koini, H.I. Kim, N. Garg, Y.F. Miura, M. Takenaga, S.S. Perry, T.R. Lee, Colloid Surf. A 154 (1999) 239.
[17] M.R. Linford, C.E.D. Chidsey, J. Am. Chem. Soc. 115 (1993) 12631.
[18] M.D. Porter, T.B. Bright, D.L. Allara, C.E.D. Chidsey, J. Am. Chem. Soc. 109 (1987) 3559.
[19] A. Ulman, J.E. Eilers, N. Tillman, Langmuir 5 (1989) 1147.
[20] B. Ewen, G.R. Strobl, D. Richter, Faraday Discuss. (1980) 19.
[21] H.Z. Yu, S. Morin, D.D.M. Wayner, P. Allongue, C.H. de Villeneuve, J. Phys. Chem. B 104 (2000) 11157.
[22] V.L. Lanza, D.B. Herrmann, J. Polym. Sci. 28 (1958) 622.
[23] C.A. Widrig, C. Chung, M.D. Porter, J. Electroanal. Chem. 310 (1991) 335.
[24] D.K. Aswal, S. Lefant, D. Guerin, J.V. Yakhmi, D. Vuillaume, Anal. Chim. Acta 568 (2006) 84.
[25] J. Cheng, D.B. Robinson, R.L. Cicero, T. Eberspacher, C.J. Bartlett, C.E.D. Chidsey, J. Phys. Chem. B 105 (2001) 10900.